Journal of Molecular Structure 1141 (2017) 594–599

Contents lists available at ScienceDirect

Journal of Molecular Structure

journal homepage: http://www.elsevier.com/locate/molstruc

# Biopolymer-mediated synthesis of $Fe_3O_4$ nanoparticles and investigation of their *in vitro* cytotoxicity effects

Aida Gholoobi [a], Zahra Meshkat [b], Khalil Abnous [c], Majid Ghayour-Mobarhan [d], Mohammad Ramezani [c], Fatemeh Homaei Shandiz [e], K.D. Verma [f], Majid Darroudi, PhD [g, *]

[a] Department of Modern Sciences and Technologies, Mashhad University of Medical Sciences, Mashhad, Iran
[b] Women's Health Research Center, Mashhad University of Medical Sciences, Mashhad, Iran
[c] Pharmaceutical Research Center, Mashhad University of Medical Sciences, Mashhad, Iran
[d] Biochemistry & Nutrition Research Center, Mashhad University of Medical Sciences, Mashhad, Iran
[e] Cancer Research Center, Mashhad University of Medical Sciences, Mashhad, Iran
[f] Material Science Research Laboratory, Department of Physics, S.V. College, Aligarh 202001, U.P., India
[g] Nuclear Medicine Research Center (NMRC), Mashhad University of Medical Sciences, Mashhad, Iran

ARTICLE INFO

*Article history:*
Received 18 February 2017
Received in revised form
10 April 2017
Accepted 10 April 2017

*Keywords:*
Superparamagnetic iron oxide nanoparticles (SPIONs)
Starch
Powder X–ray diffraction (PXRD)
Field emission scanning electron microscopy (FESEM)
*In vitro* cytotoxicity

ABSTRACT

Superparamagnetic iron oxide nanoparticles (SPIONs; $Fe_3O_4$) were synthesized by a "***green***" co-precipitation method in aqueous starch solution as a food media. Powder X-ray diffraction (PXRD) patterns indicated that the synthesized samples were pure $Fe_3O_4$ with a spinel structure, and the coating of starch did not undergo any phase change. Fourier transform infrared (FTIR) spectra confirmed the formation of starch coated $Fe_3O_4$ nanoparticles. Field emission scanning electron microscopy (FESEM) micrographs illustrated the formation of nanoparticles in the size range of below 25 nm. Magnetic measurements revealed that the saturated magnetization of the starch-SPIONs reached 36.5 emu/g. The non-toxic effect of SPIONs concentration below 50 and 100 μg/ml was observed in the studies of *in vitro* cytotoxicity on normal and cancerous cell lines, respectively. The dose dependent toxicity made it a suitable candidate for various medical applications.



## 1. Introduction

Magnetic nanoparticles are attractive materials with significant potential for use in a wide range of applications [1–4]. Superparamagnetic iron oxide nanoparticles (SPIONs), as an important member of magnetic nanoparticles family, can be used in various medical and industrial applications, such as; cancer therapy [5], drug/gene delivery [6], magnetic resonance imaging (MRI) [7], hyperthermia [8], heavy metal absorption [9], catalysts [10], pigments [11], ferro-fluids [12], etc. For various applications, a number of factors like, particle size and distribution, morphology, and physical properties (such as optical, magnetic, and electronic) are considered as significant information for the magnetic nanoparticles.

Recently, many physical and chemical methods have been developed to prepare the superparamagnetic iron oxide ($Fe_3O_4$) nanoparticles (SPIONs), such as; hydrothermal [13], solvothermal [14], *in situ* chemical oxidative polymerization [15], chemical oxidative copolymerization [16], sol–gel [17], co–precipitation [18,19], thermal decomposition [20], chemical vapor deposition (CVD) [21], electrochemical [22], microwave irradiation [23], γ–ray radiation [24], and laser ablation [25]. However, these techniques suffer the inability to control the size and distribution of SPIONs due to their large surface area, high surface energy and high magnetization which results in agglomeration and cluster formation [26]. Recently, "green"-mediated methods have also been developed for preparing the small and uniform (in size and crystalline structure) metal oxide nanoparticles [27–30] especially SPIONs [31–33]. However, many scientific studies are still underway to prepare the desired/controlled size and monodispersed SPIONs.

In this work, we report for the first time the synthesis of mono-

* Corresponding author. Nuclear Medicine Research Center (NMRC), School of Medicine, Mashhad University of Medical Sciences, Mashhad, Iran.
*E-mail addresses:* darroudim@mums.ac.ir, majiddarroudi@gmail.com (M. Darroudi).

http://dx.doi.org/10.1016/j.molstruc.2017.04.024
0022-2860/

dispersed SPIONs in soluble starch solutions using only Iron (II) chloride salt as iron precursor via a "green" co-precipitation method. Soluble starch was employed as a control sizer and/or stabilization agent to prevent uncontrollable growth and aggregation among nanoparticles. Also, To the best of our knowledge, the cytotoxicity of the prepared SPIONs towards HeLa and HNCF-PI 52 cell lines is being reported here for the first time.

## 2. Materials and methods

### 2.1. Chemicals, cell culture and maintenance

Starting materials were at analytical grade without further purification. $FeCl_2.4H_2O$ (Merck), $NH_4OH$ solution (25 vol%, Merck), and starch (Amylose molecular form, soluble, Sigma-Aldrich) were used as iron source, pH-adjusting reagent, and capping agent. Cervical cancer (HeLa) and human normal fibroblast-like cervical (HNCF-PI 52) cell lines were purchased from the Pasteur Institute (National Cell Bank of Iran). Resazurin sodium salt (AlamarBlue®) was obtained from Sigma-Aldrich (Saint Louis, MO, USA). The cells were cultured in RPMI 1640 medium containing 10% heat inactivated fetal bovine serum (Gibco), and 100 IU/ml penicillin and 100 (μg/mL) streptomycin (Invitrogen).

### 2.2. Synthesis of SPIONs

The SPIONs were synthesized via a modified green co–precipitation method, using $FeCl_2 \cdot 4H_2O$ and starch in an alkaline aqueous solution. First, 1.0 g of $FeCl_2 \cdot 4H_2O$ was dissolved in 30 ml of deionized water (DIW); then, HCl (0.50 M, 3.0 ml) was added and stirred at ambient temperature (until pH = 3 (±0.01)) for about 30 min. After addition of $NH_4OH$ solution (25%, 4.7 ml) along with continuous stirring at 70 °C for 60 min, pH of the solution was increased to 9.0 (±0.01) on precipitation process. Then, 40 ml of starch solution (2% w/w) was added to the initial solution, and the final solution was continuously stirred at 50 °C for about 90 min. The obtained precipitates were collected and washed twice with DIW/ethanol to remove the reagents such as ammonia. The obtained precipitates (black powder) were dried overnight at 100 °C.

### 2.3. Resazurin reduction assay of SPIONs

A resazurin reduction assay [34] was used to investigate the cytotoxicity of SPIONs on cervical cancer and normal cell lines. In brief, adherent cells were detached via treatment with 0.5% trypsin/EDTA and 10,000 HeLa cells, and 5000 HNCF-PI 52 cells were seeded in each well in a total volume of 200 μl standard medium. The cells were maintained as monolayer cultures at 37 °C in a humidified 5% $CO_2$ atmosphere, and were plated for 72 h prior to treatment to allow adherence. The cells were treated in various concentrations of SPIONs i.e., 0.78, 1.56, 3.125, 6.25, 12.5, 25, 50, and 100 μg/ml. After 24 h, 20 μl resazurin (0.01% w/v in DIW) was added to each well and the plates were incubated for 5 h at 37 °C. The cell viability was determined by measuring the absorbance at 570 and 600 nm in a Synergy H4 Hybrid Multi-Mode Microplate Reader (BioTek, Winooski, USA). Each experiment was performed with three replicates and the viability was analyzed based on a comparison with untreated cells.

### 2.4. Characterization of starch–SPIONs

The prepared SPIONs were characterized using XRD (Philips, X'pert, Cu $K_\alpha$, Netherlands), FE-SEM (Carl Zeiss Supra 55VP, Germany), and FTIR (Shimadzu 8400, Japan). Magnetic properties of the prepared SPIONs was measured by a vibrating sample magnetometer (VSM, AGFM/VSM 3886 Kashan, Iran) at ambient temperature in a magnetic field strength of 1.0 T.

## 3. Results and discussion

Fig. 1 shows the PXRD patterns of the obtained SPIONs. Typical peaks of SPIONs [2θ = 30.4° (220), 35.7° (311), 43.5° (400), 53.9° (422), 57.5° (511), and 63.1° (440)], were consistent with the cubic inverse spinel structure of $Fe_3O_4$ (JCPDS file No. 19–0629). As shown in the PXRD pattern, there were no other peaks for byproducts or impurities like, ferric nitrate [$Fe(NO_3)_3$], goethite [FeO(OH)], and maghemite ($\gamma$-$Fe_2O_3$). The crystallite size was calculated by the Debye–Scherrer equation ($D = K\lambda/\beta\cos\theta$), where; D is the particle size, K = 0.89, $\lambda_{(X\text{-ray wavelength})} = 0.15{,}406$ nm, β is the full width at half–maximum of diffraction peak, and θ is the X–ray diffraction angle [35]. The starch coated SPIONs presented the crystallite size of ~15 nm.

As illustrated in Fig. 2, the SPIONs are spherical in shape and are uniformly dispersed. Based on FESEM micrographs at different magnifications, we found that the obtained SPIONs were about 28 nm in mean diameter. The agglomeration of nanoparticles to some extent is due to the interaction between SPIONs.

In this work, an aqueous solution containing $Fe^{2+}$ produced a dark green precipitate immediately after being mixed with the ammonium hydroxide solution, and the obtained precipitate gradually turned black in color. Therefore, following chemical reaction (alkalization reaction) mechanism is proposed and formulated to understand the typical SPIONs formation [36]:

$$FeCl_2 \xrightarrow{\text{Hydrolysis}} Fe^{2+} + 2Cl^- \quad (1)$$

$$Fe^{2+} + 2OH^- \rightarrow Fe(OH)_2 \quad (2)$$

$$3Fe(OH)_2 + \frac{1}{2}O_2 \rightarrow Fe(OH)_2 + 2FeOOH + H_2O \quad (3)$$

$$Fe(OH)_2 + 2FeOOH \rightarrow Fe_3O_4\downarrow + 2H_2O \quad (4)$$

Thus, in this synthetic procedure, SPIONs are formed - in presence of $Fe^{2+}$ alone – due to dehydration process in Eq. (4). Goethite (FeOOH) is produced by the fractional oxidation of $Fe(OH)_2$ by dissolved oxygen gas in air (eq. (3)). This process is a controllable mechanism in transforming $Fe(OH)_2$ phases into the final phase of $Fe_3O_4$.

Fig. 3 illustrates the FTIR spectrum of the obtained starch coated SPIONs. The band centered at 3419 $cm^{-1}$ is related to –OH group (stretching mode). The typical bands of SPIONs at 435, 574, and 627 $cm^{-1}$ can be related to the Fe–O bond [37]. Characteristic bands of starch molecules were appeared at wavenumbers of 1018 and 1155 $cm^{-1}$, attributed to C–O (stretching mode) in C–O–C and C–OH groups, respectively [38]. Furthermore, the absorption bonds at about 2925 and 3419 $cm^{-1}$, were related to C–H and O–H (vibration mode) groups, respectively [39].

The magnetic behavior of as-prepared starch–SPIONs was performed by a vibrating sample magnetometry (VSM) instrument at ambient temperature. As can be seen in Fig. 4, the room-temperature magnetization curve (M–H loop) display narrow hysteresis for the starch–SPIONs revealing that the as-prepared sample in this work was a soft magnet with superparamagnetic behavior [40–42]. The starch coated SPIONs showed (Fig. 4) superparamagnetic behavior with a saturation magnetization (*Ms*) value at about 36.5 emu/g, meaning that the obtained starch–-SPIONs are suitable for medical applications such as in cell separation and magnetic resonance imaging (MRI) [43,44]. The value

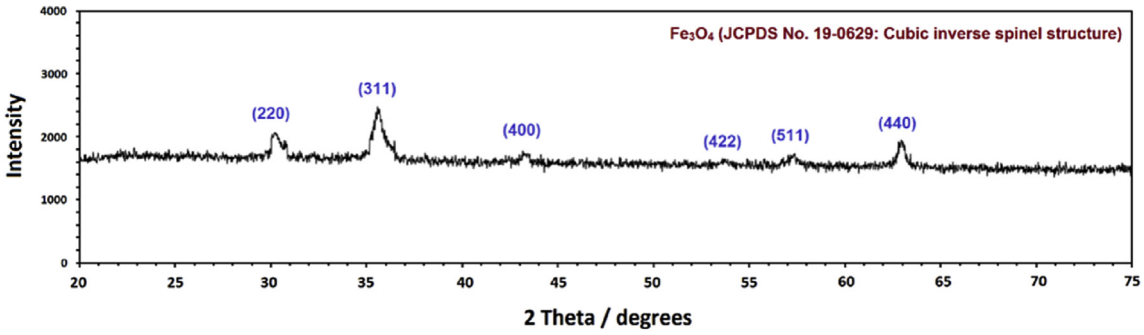


**Fig. 1.** PXRD pattern of prepared starch–SPIONs.

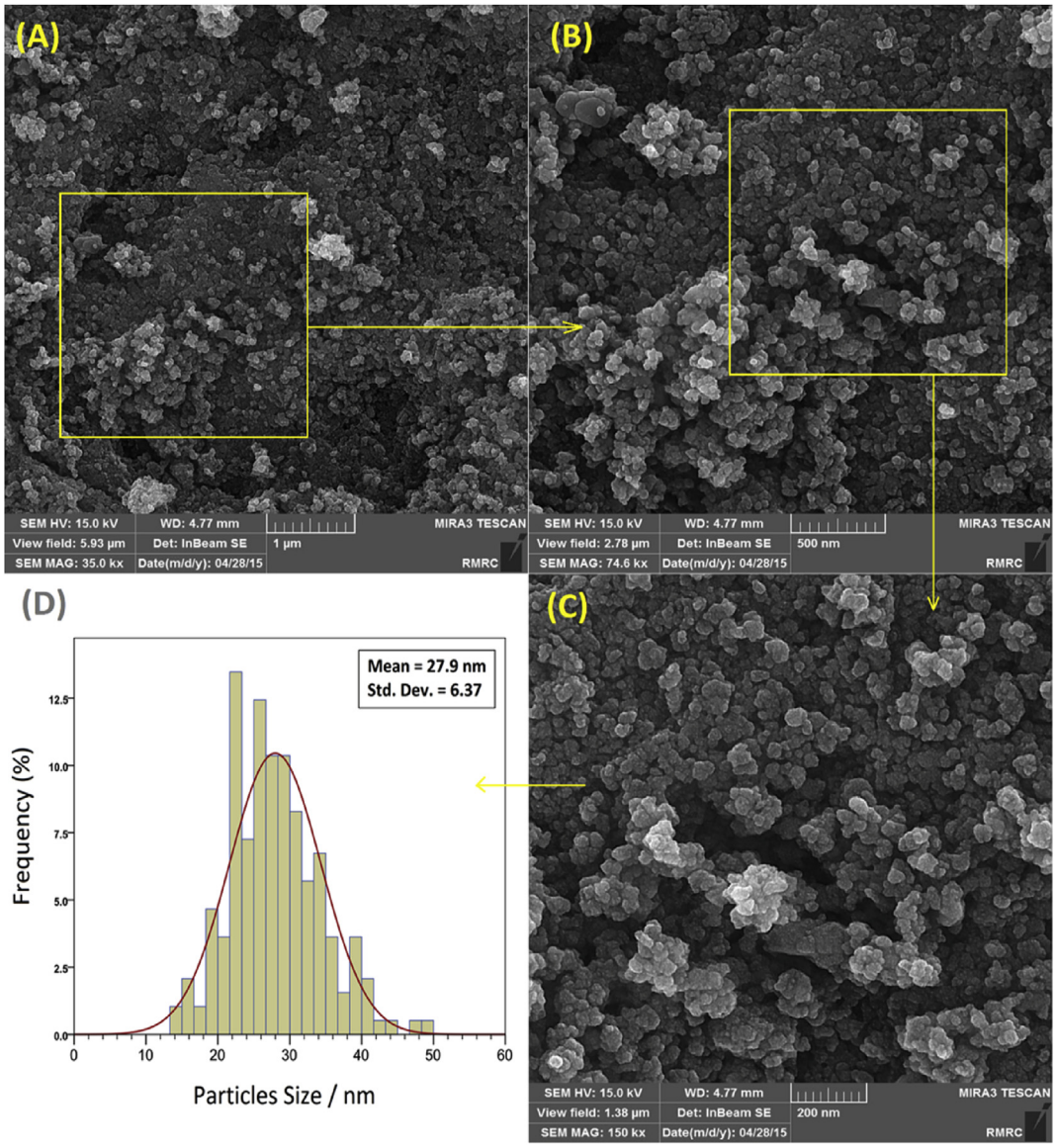


**Fig. 2.** FESEM micrographs of prepared starch–SPIONs at different magnification (A: × 35,000, B: × 75,000 and C: × 150,000) and a typical size distribution (D).

obtained from magnetization measurement is in moral agreement with the literature [45,46]. The decrease of *Ms* value for starch-SPIONs (in comparison with bulk $Fe_3O_4$ ~85–100 emu/g) can be related to a number of factors including cation distribution, surface disorder, and particle size decrease. Normally, the decrease in size of particle (from bulk to nanoparticles) causes the increase of the surface area that it results in the decrease of *Ms* value compared to that of bulk magnetite material due to the decrease of the effective magnetic moments [47,48].

As shown if Fig. 5, the cytotoxicity effects of the synthesized

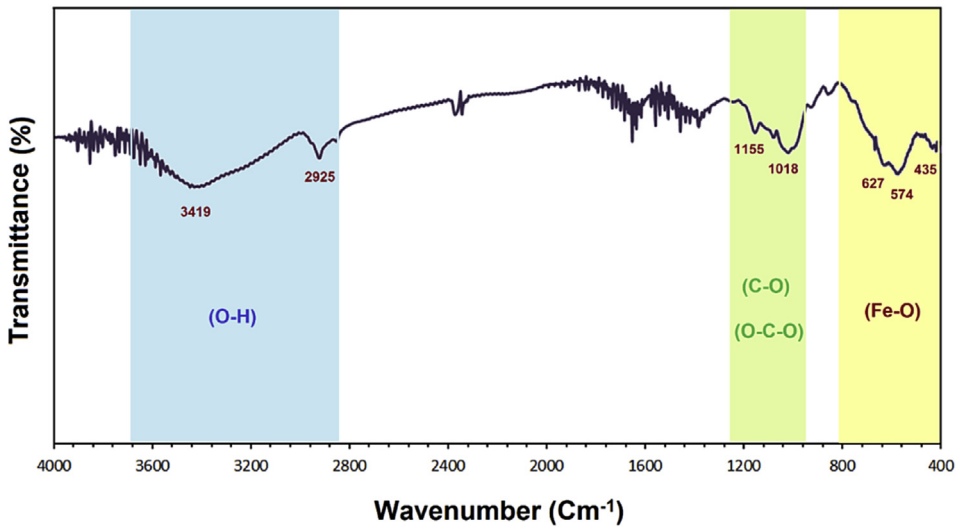


**Fig. 3.** The FTIR spectrum of starch–SPIONs.

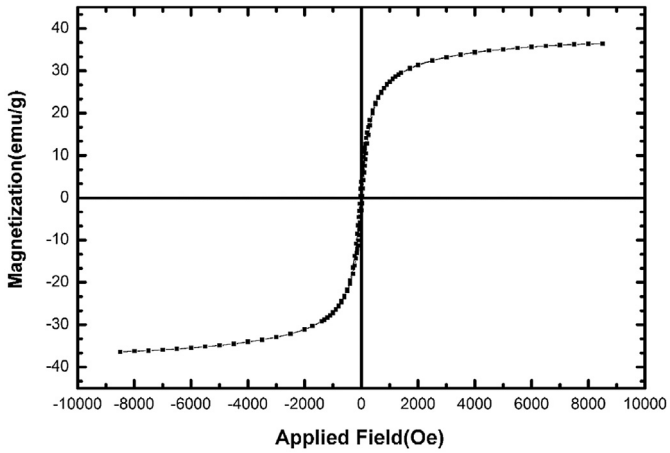


**Fig. 4.** Magnetization plot of synthesized starch–SPIONs.

SPIONs were investigated on HNCF-PI 52 and HeLa cell lines as normal and cancerous cell lines, respectively. The cells were treated with the SPIONs at various concentrations (0–100 μg/ml) for 24 h and incubated at 37 °C in a 5% $CO_2$ atmosphere. After 24 h of treatment, the *in vitro* cytotoxicity investigations revealed that the starch coated SPIONs had no toxic effect on cancerous (HeLa; 100 μg/ml) cell lines in higher concentrations (Fig. 5a). The prepared starch-coated SPIONs also demonstrated no significant toxicity even in concentrations up to 50 μg/ml on normal cell lines in the resazurin reduction assay, meaning that the SPIONs are well tolerated by HNCF-PI 52 cells (Fig. 5b).

The non-cytotoxic effect of bio-functional nanoparticles on cancer cell lines have been reported previously [49–51]. In a previous study Khullar et al., were evaluated BSA coated gold nanoparticles for cytotoxicity towards rat glioma cell line and blood cells. The nanogolds did not have cytotoxic and hemolytic response against these cells whereas BSA free nanoparticles showed low cell viability and high hemolytic activity. In another study, bio-functional nanoparticles coated with DEAE–BSA and DEAE–Lys complexes did not show any marked hemolysis activity [50]. These results are in consistent with our work which demonstrated the possibility of these nanoparticles for different biomedical applications.

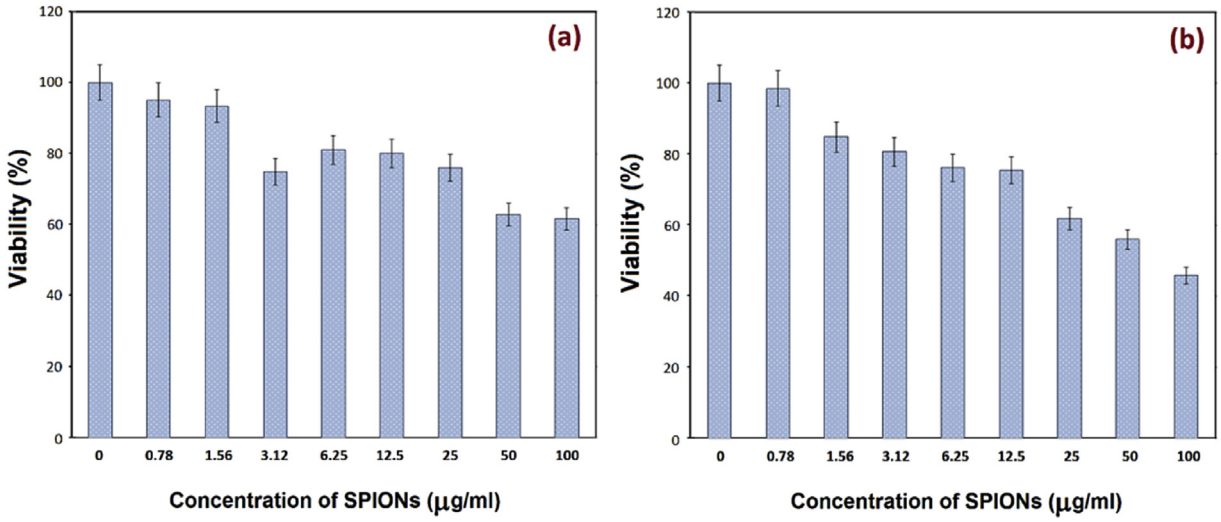


**Fig. 5.** Cytotoxicity effects of synthesized starch–SPIONs on HeLa (a) and HNCF-PI 52 (b) cell lines.

## 4. Conclusion

The SPIONs were successfully synthesized in an aqueous starch solution via a "*green*" co–precipitation method. Starch molecules were used as the capping agent (size reducing agent) and organic shell to obtain the organic–inorganic nanomaterials. The mean diameters of the SPIONs were below 25 nm with suitable superparamagnetic properties (with an *Ms* equal to 36.5 emu/g). Moreover, the starch coated SPIONs have non-toxic effects on normal and cancerous cervical cell lines, making them suitable candidates for various biological applications.

## Acknowledgments

The authors gratefully acknowledge the financial support for this work provided by Mashhad University of Medical Sciences (Grant number 910808) based on the PhD thesis (No. A-517) of Mrs. Aida Gholoobi.

## References

[1] J. Wan, W. Cai, X. Meng, E. Liu, Monodisperse water-soluble magnetite nanoparticles prepared by polyol process for high-performance magnetic resonance imaging, Chem. Commun. 47 (2007) 5004–5006.
[2] S. Mirsadeghi, S. Shanehsazzadeh, F. Atyabi, R. Dinarvand, Effect of PEGylated superparamagnetic iron oxide nanoparticles (SPIONs) under magnetic field on amyloid beta fibrillation process, Mater. Sci. Eng. C 59 (2016) 390–397.
[3] K.R. Reddy, B.C. Sin, C.H. Yoo, W. Park, K.S. Ryu, J.-S. Lee, D. Sohn, Y. Lee, A new one-step synthesis method for coating multi-walled carbon nanotubes with cuprous oxide nanoparticles, Scr. Mater. 58 (11) (2008) 1010–1013.
[4] K.R. Reddy, K.-P. Lee, A.I. Gopalan, Self-assembly directed synthesis of poly (ortho-toluidine)-metal (gold and palladium) composite nanospheres, J. Nanosci. Nanotechnol. 7 (9) (2007) 3117–3125.
[5] A.A. Kuznetsov, V.I. Filippov, R.N. Alyautdin, N.L. Torshina, O.A. Kuznetsov, Application of magnetic liposomes for magnetically guided transport of muscle relaxants and anti-cancer photodynamic drugs, J. Magn. Magn. Mater. 225 (1–2) (2001) 95–100.
[6] Y. Ding, S.Z. Shen, H. Sun, K. Sun, F. Liu, Y. Qi, J. Yan, Design and construction of polymerized-chitosan coated Fe3O4 magnetic nanoparticles and its application for hydrophobic drug delivery, Mater. Sci. Eng. C 48 (2015) 487–498.
[7] F.Q. Hu, L. Wei, Z. Zhou, Y.L. Ran, Z. Li, M.Y. Gao, Preparation of biocompatible magnetite nanocrystals for In Vivo magnetic resonance detection of cancer, Adv. Mater. 18 (19) (2006) 2553–2556.
[8] K. Hayashi, M. Nakamura, W. Sakamoto, T. Yogo, H. Miki, S. Ozaki, M. Abe, T. Matsumoto, K. Ishimura, Superparamagnetic nanoparticle clusters for cancer theranostics combining magnetic resonance imaging and hyperthermia treatment, Theranostics 3 (6) (2013) 366–376.
[9] H.-L. Fan, L. Li, S.-F. Zhou, Y.-Z. Liu, Continuous preparation of $Fe_3O_4$ nanoparticles combined with surface modification by L-cysteine and their application in heavy metal adsorption, Ceram. Int. 42 (3) (2016) 4228–4237.
[10] L.M. Rossi, F.P. Silva, L.L.R. Vono, P.K. Kiyohara, E.L. Duarte, R. Itri, R. Landers, G. Machado, Superparamagnetic nanoparticle-supported palladium: a highly stable magnetically recoverable and reusable catalyst for hydrogenation reactions, Green Chem. 9 (4) (2007) 379–385.
[11] J. Meng, G. Yang, L. Yan, X. Wang, Synthesis and characterization of magnetic nanometer pigment $Fe_3O_4$, Dyes Pigments 66 (2) (2005) 109–113.
[12] N. Mohamad Nor, K. Abdul Razak, S.C. Tan, R. Noordin, Properties of surface functionalized iron oxide nanoparticles (ferrofluid) conjugated antibody for lateral flow immunoassay application, J. Alloys Compd. 538 (2012) 100–106.
[13] H. Hashimoto, K. Higuchi, H. Inada, Y. Okazaki, T. Takaishi, H. Asoh, Well-dispersed α-$Fe_2O_3$ particles for lead-free red overglaze enamels through hydrothermal treatment, ACS Omega 1 (1) (2016) 9–13.
[14] G. Demazeau, Solvothermal reactions: an original route for the synthesis of novel materials, J. Mater. Sci. 43 (7) (2008) 2104–2114.
[15] K.R. Reddy, W. Park, B.C. Sin, J. Noh, Y. Lee, Synthesis of electrically conductive and superparamagnetic monodispersed iron oxide-conjugated polymer composite nanoparticles by in situ chemical oxidative polymerization, J. Colloid Interface Sci. 335 (1) (2009) 34–39.
[16] K.R. Reddy, K.P. Lee, A.I. Gopalan, Novel electrically conductive and ferromagnetic composites of poly (aniline-co-aminonaphthalenesulfonic acid) with iron oxide nanoparticles: synthesis and characterization, J. Appl. Polym. Sci. 106 (2) (2007) 1181–1191.
[17] M. Tadić, V. Kusigerski, D. Marković, M. Panjan, I. Milošević, V. Spasojević, Highly crystalline superparamagnetic iron oxide nanoparticles (SPION) in a silica matrix, J. Alloys Compd. 525 (2012) 28–33.
[18] C.-C. Lin, J.-M. Ho, Structural analysis and catalytic activity of $Fe_3O_4$ nanoparticles prepared by a facile co-precipitation method in a rotating packed bed, Ceram. Int. 40 (7, Part B) (2014) 10275–10282.
[19] K.R. Reddy, K.-P. Lee, J.Y. Kim, Y. Lee, Self-assembly and graft polymerization route to monodispersed $Fe_3O_4$@ $SiO_2$—polyaniline core–shell composite nanoparticles: physical properties, J. Nanosci. Nanotechnol. 8 (11) (2008) 5632–5639.
[20] Y. Zhu, F.Y. Jiang, K. Chen, F. Kang, Z.K. Tang, Size-controlled synthesis of monodisperse superparamagnetic iron oxide nanoparticles, J. Alloys Compd. 509 (34) (2011) 8549–8553.
[21] V. Sivakov, C. Petersen, C. Daniel, H. Shen, F. Mücklich, S. Mathur, Laser induced local and periodic phase transformations in iron oxide thin films obtained by chemical vapour deposition, Appl. Surf. Sci. 247 (1–4) (2005) 513–517.
[22] F. Fajaroh, H. Setyawan, W. Widiyastuti, S. Winardi, Synthesis of magnetite nanoparticles by surfactant-free electrochemical method in an aqueous system, Adv. Powder Technol. 23 (3) (2012) 328–333.
[23] A.O. Elizabeth, M.A. Tonya, A.G. Dustin, M.K. Susan, L. Kai, Y.L. Angelique, Rapid microwave-assisted synthesis of dextran-coated iron oxide nanoparticles for magnetic resonance imaging, Nanotechnology 23 (21) (2012) 215602.
[24] L.S. Darken, R.W. Gurry, The system iron—oxygen. II. Equilibrium and thermodynamics of liquid oxide and other phases, J. Am. Chem. Soc. 68 (5) (1946) 798–816.
[25] Y. Guo, Z. Zhang, D.-H. Kim, W. Li, J. Nicolai, D. Procissi, Y. Huan, G. Han, R.A. Omary, A.C. Larson, Photothermal ablation of pancreatic cancer cells with hybrid iron-oxide core gold-shell nanoparticles, Int. J. Nanomed. 8 (2013) 3437–3446.
[26] S. Ahmad, U. Riaz, A. Kaushik, J. Alam, Soft template synthesis of super paramagnetic Fe3O4 nanoparticles a novel technique, J. Inorg. Organomet. Polym. 19 (3) (2009) 355–360.
[27] M. Darroudi, M. Sarani, R. Kazemi Oskuee, A. Khorsand Zak, M.S. Amiri, Nanoceria: gum mediated synthesis and in vitro viability assay, Ceram. Int. 40 (2) (2014) 2863–2868.
[28] M. Ristic, S. Krehula, M. Reissner, M. Jean, B. Hannoyer, S. Musić, Synthesis and properties of precipitated cobalt ferrite nanoparticles, J. Mol. Struct..
[29] A.H. Atta, M.A. El-ghamry, A. Hamzaoui, M.S. Refat, Synthesis and spectroscopic investigations of iron oxide nano-particles for biomedical applications in the treatment of cancer cells, J. Mol. Struct. 1086 (2015) 246–254.
[30] B. Afzalian Mend, M. Delavar, M. Darroudi, CdO-NPs; Synthesis from 1D new nano Cd coordination polymer, characterization and application as anti-cancer drug for reducing the viability of cancer cells, J. Mol. Struct. 1134 (2017) 599–605.
[31] M. Abbas, B. Parvatheeswara Rao, S.M. Naga, M. Takahashi, C. Kim, Synthesis of high magnetization hydrophilic magnetite ($Fe_3O_4$) nanoparticles in single reaction—surfactantless polyol process, Ceram. Int. 39 (7) (2013) 7605–7611.
[32] J. Qu, G. Liu, Y. Wang, R. Hong, Preparation of $Fe_3O_4$–chitosan nanoparticles used for hyperthermia, Adv. Powder Technol. 21 (4) (2010) 461–467.
[33] S. Groiss, R. Selvaraj, T. Varadavenkatesan, R. Vinayagam, Structural characterization, antibacterial and catalytic effect of iron oxide nanoparticles synthesised using the leaf extract of Cynometra ramiflora, J. Mol. Struct. 1128 (2017) 572–578.
[34] J. O'Brien, I. Wilson, T. Orton, F. Pognan, Investigation of the Alamar Blue (resazurin) fluorescent dye for the assessment of mammalian cell cytotoxicity, Eur. J. Biochem. 267 (17) (2000) 5421–5426.
[35] M. Nidhin, R. Indumathy, K.J. Sreeram, B. Nair, Synthesis of iron oxide nanoparticles of narrow size distribution on polysaccharide templates, Bull. Mater. Sci. 31 (1) (2008) 93–96.
[36] A.A. Olowe, J.M.R. Génin, The mechanism of oxidation of ferrous hydroxide in sulphated aqueous media: importance of the initial ratio of the reactants, Corros. Sci. 32 (9) (1991) 965–984.
[37] D. Dorniani, M.Z.B. Hussein, A.U. Kura, S. Fakurazi, A.H. Shaari, Z. Ahmad, Preparation of Fe(3)O(4) magnetic nanoparticles coated with gallic acid for drug delivery, Int. J. Nanomed. 7 (2012) 5745–5756.
[38] A. Khorsand Zak, W.H. Abd Majid, M.R. Mahmoudian, M. Darroudi, R. Yousefi, Starch-stabilized synthesis of ZnO nanopowders at low temperature and optical properties study, Adv. Powder Technol. 24 (3) (2013) 618–624.
[39] Y.F. Shen, J. Tang, Z.H. Nie, Y.D. Wang, Y. Ren, L. Zuo, Preparation and application of magnetic $Fe_3O_4$ nanoparticles for wastewater purification, Sep. Purif. Technol. 68 (3) (2009) 312–319.
[40] D.-H. Chen, M.-H. Liao, Preparation and characterization of YADH-bound magnetic nanoparticles, J. Mol. Catal. B Enzym. 16 (5) (2002) 283–291.
[41] M.Y. Ghotbi, M.Z. bin Hussein, Controlled release study of an anti-carcinogenic agent, gallate from the surface of magnetite nanoparticles, J. Phys. Chem. Solids 73 (7) (2012) 936–942.
[42] P.A. Dresco, V.S. Zaitsev, R.J. Gambino, B. Chu, Preparation and properties of magnetite and polymer magnetite nanoparticles, Langmuir 15 (6) (1999) 1945–1951.
[43] K.C. Barick, S. Singh, D. Bahadur, M.A. Lawande, D.P. Patkar, P.A. Hassan, Carboxyl decorated $Fe_3O_4$ nanoparticles for MRI diagnosis and localized hyperthermia, J. Colloid Interface Sci. 418 (2014) 120–125.
[44] R.Y. Hong, B. Feng, L.L. Chen, G.H. Liu, H.Z. Li, Y. Zheng, D.G. Wei, Synthesis, characterization and MRI application of dextran-coated $Fe_3O_4$ magnetic nanoparticles, Biochem. Eng. J. 42 (3) (2008) 290–300.
[45] M. Mandal, S. Kundu, S.K. Ghosh, S. Panigrahi, T.K. Sau, S. Yusuf, T. Pal, Magnetite nanoparticles with tunable gold or silver shell, J. Colloid Interface Sci. 286 (1) (2005) 187–194.
[46] Y.-Q. Zhang, X.-W. Wei, R. Yu, $Fe_3O_4$ Nanoparticles-supported palladium-

bipyridine complex: effective catalyst for suzuki coupling reaction, Catal. Lett. 135 (3–4) (2010) 256–262.
[47] L. Zhao, H. Zhang, Y. Xing, S. Song, S. Yu, W. Shi, X. Guo, J. Yang, Y. Lei, F. Cao, Morphology-controlled synthesis of magnetites with nanoporous structures and excellent magnetic properties, Chem. Mater. 20 (1) (2007) 198–204.
[48] Z. Lu, W. Zou, L. Lv, X. Liu, S. Li, J. Zhu, F. Zhang, Y. Du, Large low-field magnetoresistance in nanocrystalline magnetite prepared by sol-gel method, J. Phys. Chem. B 110 (47) (2006) 23817–23820.
[49] P. Khullar, V. Singh, A. Mahal, P.N. Dave, S. Thakur, G. Kaur, J. Singh, S. Singh Kamboj, M. Singh Bakshi, Bovine serum albumin bioconjugated gold nanoparticles: synthesis, hemolysis, and cytotoxicity toward cancer cell lines, J. Phys. Chem. C 116 (15) (2012) 8834–8843.
[50] M.K. Goshisht, L. Moudgil, P. Khullar, G. Singh, A. Kaura, H. Kumar, G. Kaur, M.S. Bakshi, Surface adsorption and molecular modeling of biofunctional gold nanoparticles for systemic circulation and biological sustainability, ACS Sustain. Chem. Eng. 3 (12) (2015) 3175–3187.
[51] S. Vijayakumar, S. Ganesan, In vitro cytotoxicity assay on gold nanoparticles with different stabilizing agents, J. Nanomater. 2012 (2012) 9.